

Supplementary Information

Title

Membrane-anchoring stabilizes and favors secretion of New Delhi Metallo- β -lactamase

Authors

Lisandro J. González¹, Guillermo Bahr¹, Toshiki G. Nakashige², Elizabeth M. Nolan², Robert A. Bonomo³ and Alejandro J. Vila^{1*}

Affiliations

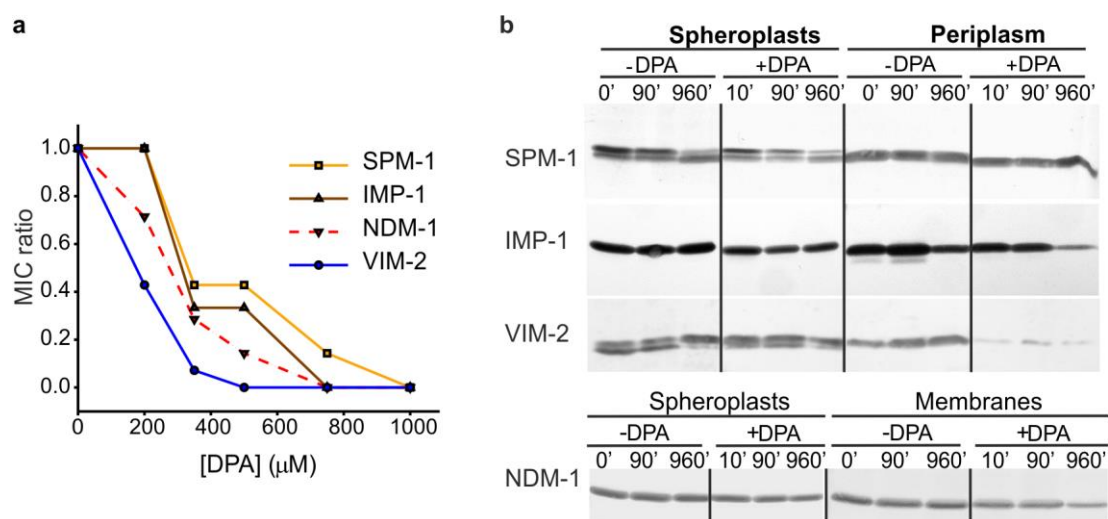
¹Instituto de Biología Molecular y Celular de Rosario (IBR, CONICET-UNR) and Área Biofísica, Facultad de Ciencias Bioquímicas y Farmacéuticas, Universidad Nacional de Rosario, Rosario, Argentina

²Department of Chemistry, Massachusetts Institute of Technology, Cambridge, Massachusetts 02139, USA

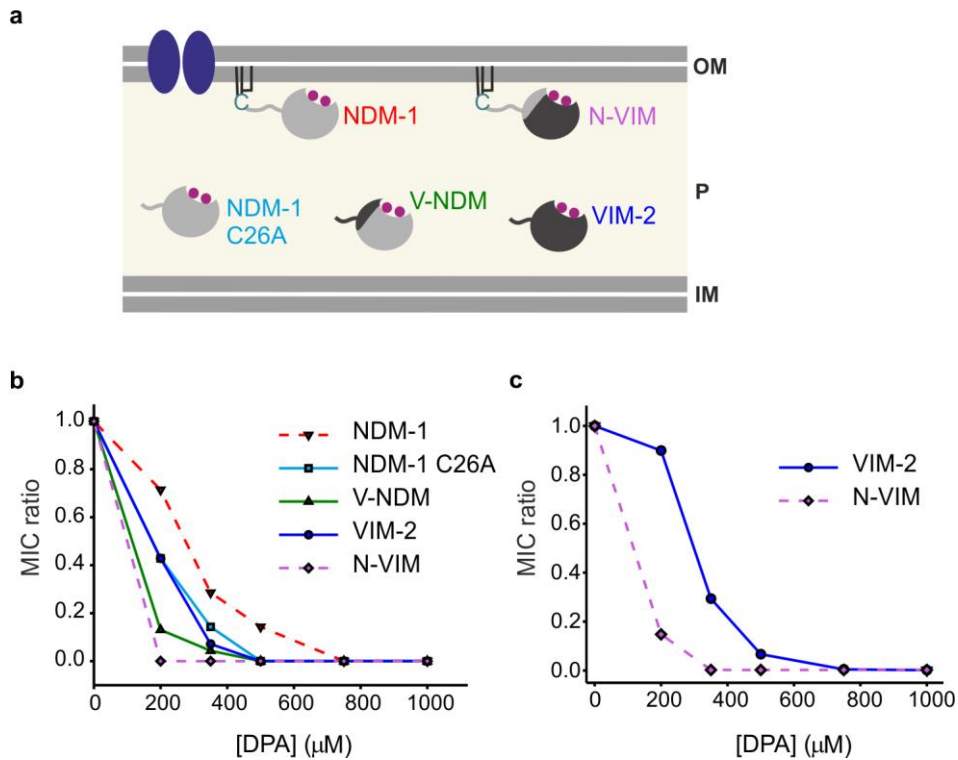
³Research Service, Louis Stokes Cleveland Department of Veterans Affairs Medical Center, Cleveland, OH; Departments of Medicine, Pharmacology, Microbiology and Molecular Biology; Case Western Reserve University, Cleveland, OH, USA

*Corresponding author. E-mail: vila@ibr-conicet.gov.ar

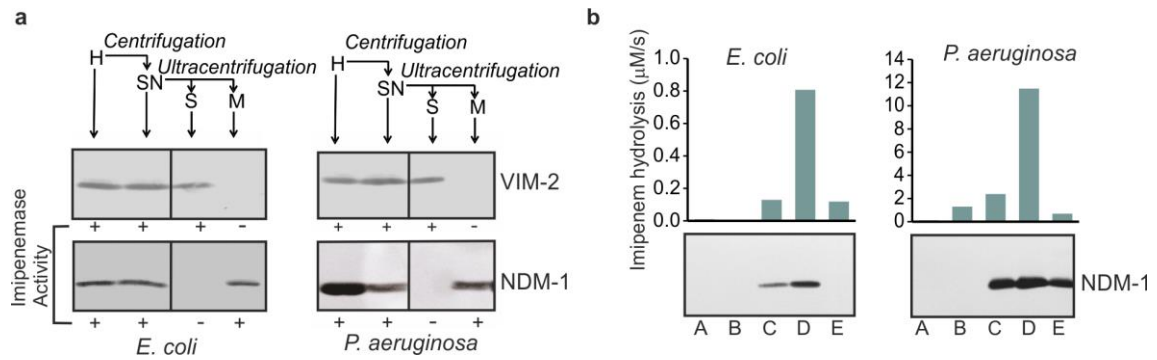
Supplementary Results



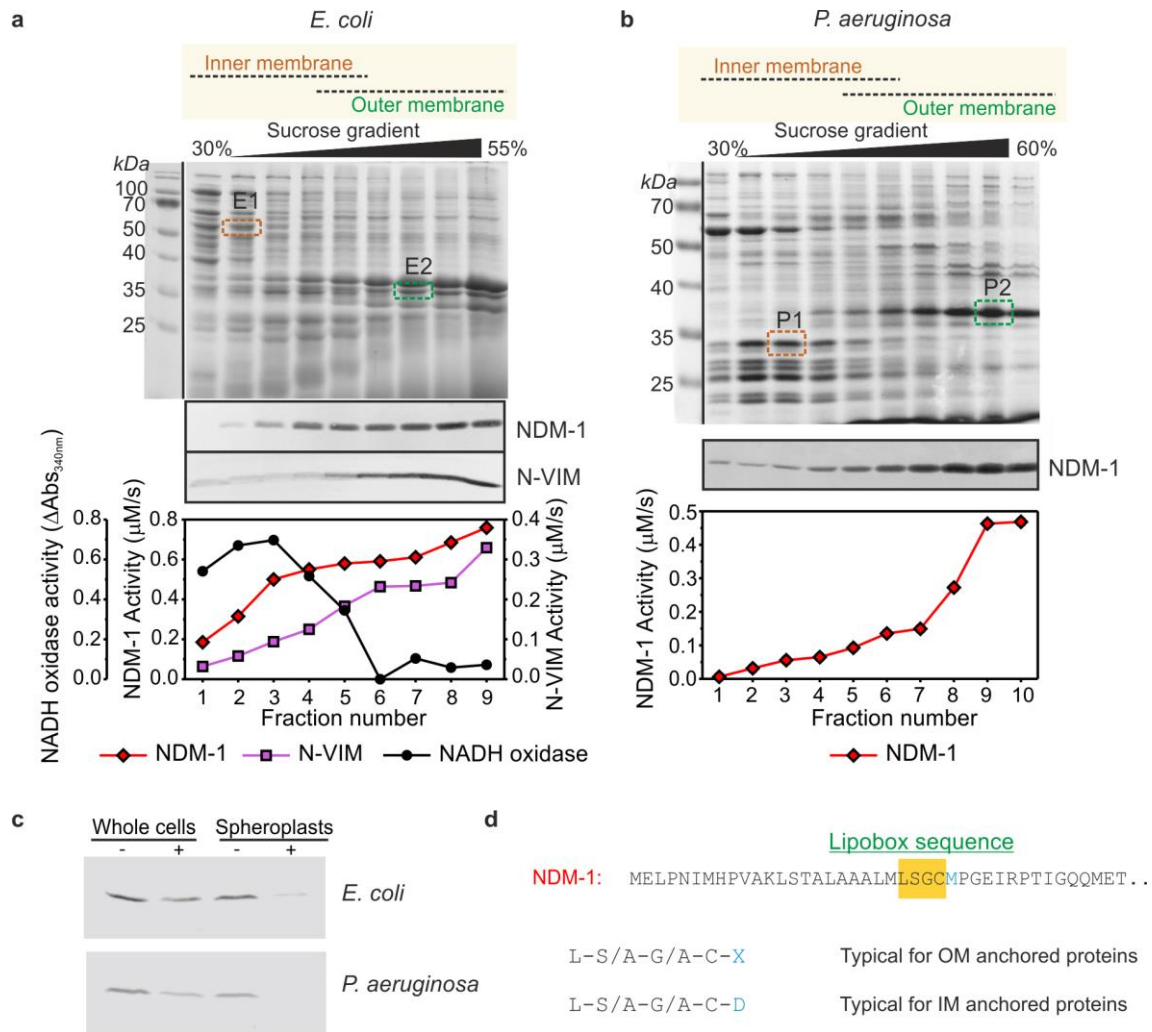
Supplementary Figure 1. Effect of Zn(II) availability on β -lactam resistance and MBL levels. (a) Relative MIC values of imipenem for *E. coli* cells expressing SPM-1, IMP-1, NDM-1 or VIM-2 in growth medium supplemented with different concentrations of the metal chelator DPA. MIC ratio values were calculated as described in the Methods section. Data correspond to three independent determinations, with standard errors $\leq 16\%$ of each data point. (b) MBL levels in different cellular fractions as a function of time after addition of 1000 μM DPA. Equal amounts of total proteins were loaded on gels for each sample. Full Western Blots are displayed in Supplementary Fig. 12.



Supplementary Figure 2. Effect of Zn(II) availability on β -lactam MICs of *E. coli* strains expressing different MBLs and variants. (a) Schematic representation of the cellular localization of NDM-1, NDM-1 C26A, V-NDM, VIM-2 and N-VIM variants (see Supplementary Figure S4 for further details). (b) Relative MIC values of imipenem for *E. coli* cells expressing NDM-1, VIM-2, NDM-1 C26A, V-NDM and N-VIM variants in growth medium supplemented with different concentrations of DPA. (c) Relative MICs values of cefotaxime for *E. coli* cells expressing wild-type VIM-2 or N-VIM in growth medium supplemented with different concentrations of DPA. MIC ratio values were calculated as described in the Methods section. Data correspond to three independent determinations, with standard errors $\leq 16\%$ of each data point.

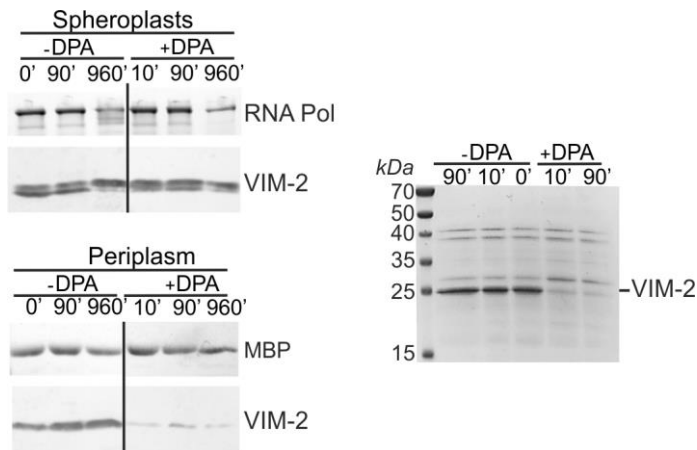


Supplementary Figure 3. NDM-1 is bound to the bacterial membranes of *E. coli* and *P. aeruginosa* through hydrophobic interactions. (a) Western blot detection of NDM-1 or VIM-2 in different cell fractions of *E. coli* or *P. aeruginosa*. After growth, cells were disrupted by sonication. The resulting homogenate (H) was then centrifuged 10 min at 12,800xg at 4°C to remove cell debris, and a supernatant (SN) was separated. Soluble cells contents (S) and membrane vesicles (M) present in this fraction were separated through ultracentrifugation at 150,000xg 4°C for 1 h. NDM-1 is a membrane-associated protein in both hosts, whereas VIM-2 is a soluble periplasmic MBL. (b) Membrane preparations of *E. coli* and *P. aeruginosa* expressing NDM-1. Membranes were sequentially treated with different reagents to determine the type of interaction that binds NDM-1 to membranes: (A) KCl 1M, (B) Na₂CO₃ 0.1 M, (C) Triton X-100 0.0016% w/v, (D) Triton X-100 0.23% w/v and (E) remaining membranes after final treatment. Solubilization of NDM-1 after each step was analyzed by Western blot and imipenem hydrolysis. The results show that NDM-1 is extracted only in the presence of Triton X-100, indicating that this MBL is bound to bacterial membranes through hydrophobic interactions. Full Western Blots are displayed in Supplementary Fig. 12.



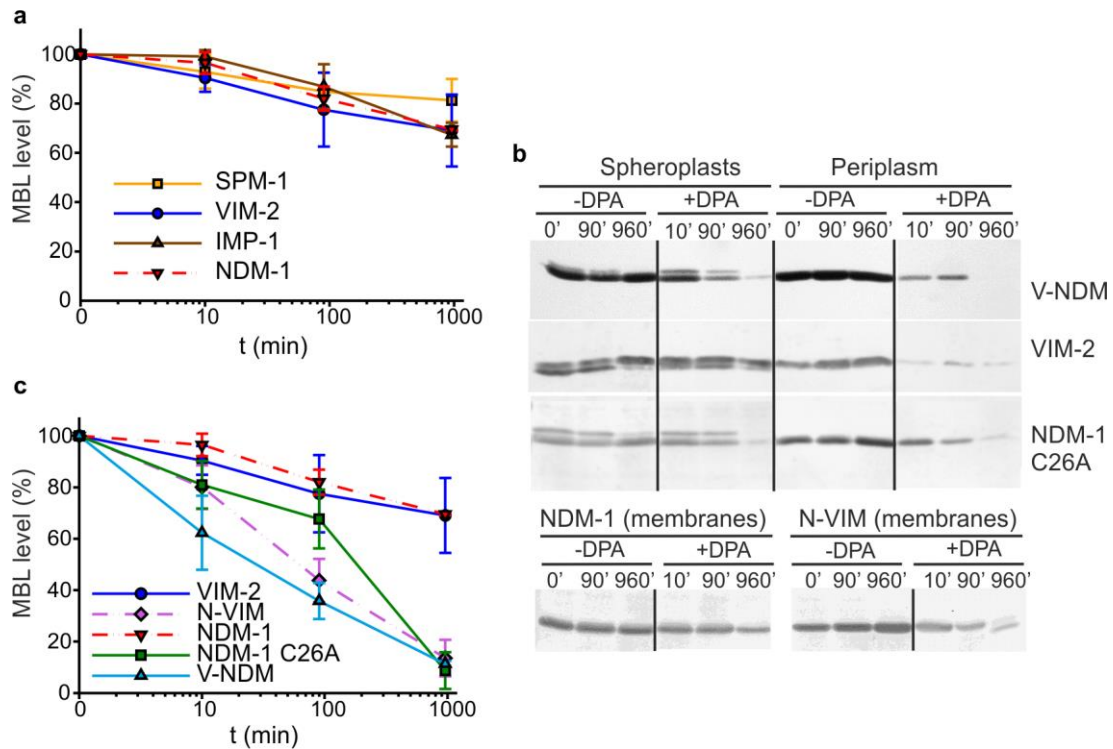
Supplementary Figure 4. Localization and orientation of NDM-1 and N-VIM within the bacterial outer membrane. (a) Membranes from *E. coli* expressing NDM-1 or N-VIM were subjected to ultracentrifugation in a 30 to 55% w/v sucrose gradient for separation of outer (OM) and inner (IM) membranes. Fractions along the gradient were analyzed by SDS-PAGE and Western blot detection of NDM-1 and N-VIM (anti StrepTag antibodies), imipenemase and NADH oxidase activity. In addition, protein bands highlighted with rectangles were excised from the gels and analyzed by mass spectrometry to confirm the OM (green) or IM (orange) character of the fractions (E1, protein-export membrane protein SecD; E2, OmpA). NDM-1 is concentrated in the OM fractions from both bacterial hosts, indicating OM localization. (b) Separation of OM and IM fractions from *P. aeruginosa* expressing NDM-1 along a 30 to 60% w/v sucrose gradient. OM or IM character was determined by mass spectrometry of excised bands

(P1, ATP synthase subunit b and Signal Peptidase I; P2, OmpF), and the presence of NDM-1 was detected as in (a). (c) Whole cells (W) and permeable spheroplasts (S) of *E. coli* and *P. aeruginosa* expressing NDM-1 were subjected to limited proteolysis with proteinase K. Comparison of NDM-1 levels detected by Western blot in protease treated samples (+) versus untreated controls (–) shows that NDM-1 is resistant to proteolysis in whole cells, while being degraded in spheroplasts under identical conditions. These results demonstrate that NDM-1 is inaccessible to external proteases, and thus located in the inner leaflet of the outer membrane. (d) The N-terminus of NDM-1 contains a canonical lipobox sequence (highlighted in orange), which includes a cysteine residue that undergoes lipidation followed by peptide leader processing in the bacterial IM¹. The identity of the residue immediately posterior to the C terminal end of posterior the lipobox determines whether the lipoprotein will be localized to IM or OM, with an aspartic acid being required for retention in IM. The presence of a methionine residue at this position in NDM-1 is suggestive of targeting to the OM. Full Western Blots are displayed in Supplementary Fig. 12.

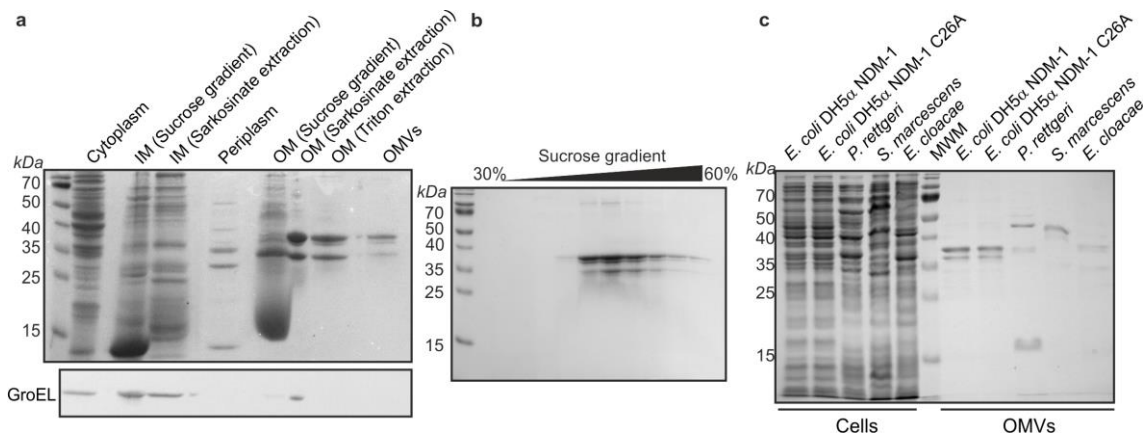


Supplementary Figure 5. Zn(II) deprivation causes selective degradation of MBLs

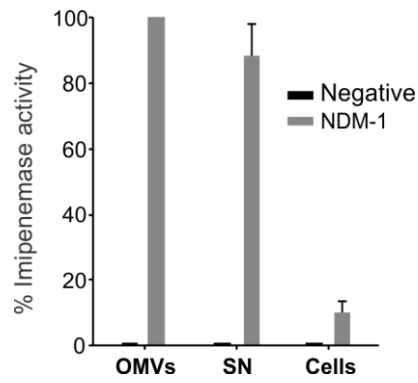
in the periplasm. Left, immunodetection of VIM-2 in spheroplasts and periplasmic extracts of *E. coli* cells exposed to 1000 μ M DPA (or no DPA) at 20°C for different time-periods. Western blots of periplasmic maltose binding protein (MBP) and cytoplasmic RNA polymerase (RNA pol) were performed as loading controls for periplasmic extracts and spheroplasts, respectively. Right, Coomassie-stained SDS-PAGE of periplasmic extracts. There is a clear and selective reduction in the intensity of the band corresponding to VIM-2. The rest of the protein pattern remains unchanged. Full Western Blots are displayed in Supplementary Figs. 12 and 13.



Supplementary Figure 6. Protein levels of MBLs in different cellular fractions under conditions of Zn(II) deprivation. (a) Spheroplast MBL levels (full-length and processed forms) determined by Western blot from *E. coli* expressing SPM-1, VIM-2, IMP-1 or NDM-1 at different times after addition of 1000 μ M DPA. (b) MBL levels of NDM-1, VIM-2 and related mutants in periplasm and spheroplasts as a function time after addition of 1000 μ M DPA. Full Western Blots are displayed in Supplementary Figs. 12 and 13. (c) Spheroplast MBL levels determined by Western blot from *E. coli* cultures VIM-2, N-VIM, NDM-1, NDM-1 C26A or V-NDM at different times after addition of 1000 μ M DPA. Data correspond to three independent experiments and are shown as mean \pm s.e.m.



Supplementary Figure 7. Purification and quality control of OMVs. (a) Subcellular fractions from *E. coli* cells expressing NDM-1 were analyzed by SDS-PAGE and Western blot with anti-GroEL antibodies. Full Western Blot is displayed in Supplementary Fig. 13. (b) OMVs purified from *E. coli* expressing NDM-1 were subjected to ultracentrifugation in a 30 to 60% w/v sucrose gradient, and fractions along the gradient were analyzed by SDS-PAGE. (c) Whole cell extracts and OMVs purified from *E. coli* expressing NDM-1 or NDM-1 C26A, and three clinical isolates expressing NDM-1, were analyzed by SDS-PAGE.



Supplementary Figure 8. NDM-1 OMVs endow cells with β -lactamase activity.

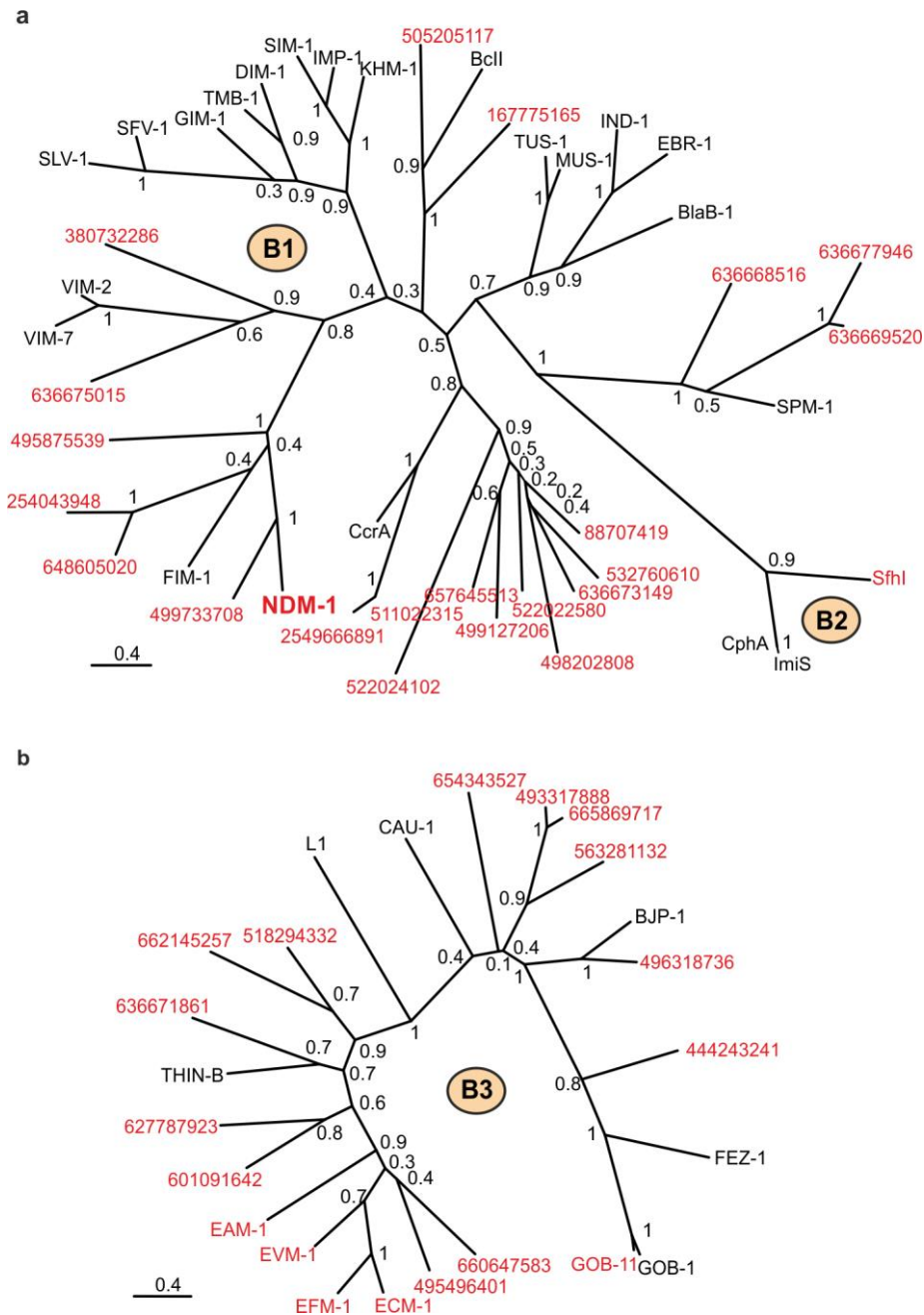
Imipenemase activity of β -lactam sensitive *E. coli* cells after incubation with 8 μ g of NDM-1-containing (NDM-1) or non-MBL-producing OMVs (Negative), compared to OMVs and supernatant (SN) obtained after pelleting cells. Imipenem hydrolysis rates of SN and Cells were measured and normalized to OMVs for comparison. Data correspond to three independent experiments and are shown as mean \pm s.e.m.

```

NDM-1 1 MELPNIMHPVAKLSTALAAALM LSGC MPGEIRPTIGQQMETGDQRFGDL 49
NDM-2 1 MELPNIMHPVAKLSTALAAALM LSGC MAGEIRPTIGQQMETGDQRFGDL 49
NDM-3 1 MELPNIMHPVAKLSTALAAALM LSGC MPGEIRPTIGQQMETGDQRFGDL 49
NDM-4 1 MELPNIMHPVAKLSTALAAALM LSGC MPGEIRPTIGQQMETGDQRFGDL 49
NDM-5 1 MELPNIMHPVAKLSTALAAALM LSGC MPGEIRPTIGQQMETGDQRFGDL 49
NDM-6 1 MELPNIMHPVAKLSTALAAALM LSGC MPGEIRPTIGQQMETGDQRFGDL 49
NDM-7 1 MELPNIMHPVAKLSTALAAALM LSGC MPGEIRPTIGQQMETGDQRFGDL 49
NDM-8 1 MELPNIMHPVAKLSTALAAALM LSGC MPGEIRPTIGQQMETGDQRFGDL 49
NDM-9 1 MELPNIMHPVAKLSTALAAALM LSGC MPGEIRPTIGQQMETGDQRFGDL 49
NDM-10 1 MELPNIMHPVAKLSTALAAALM LSGC MPGEISPTIDQQMETGDQRFGDL 49
NDM-11 1 MELPNIMHPVAKLSTALAAALM LSGC MPGEIRPTIGQQMETGDQRFGDL 49
NDM-12 1 MELPNIMHPVAKLSTALAAALM LSGC MPGEIRPTIGQQMETGDQRFGDL 49
NDM-13 1 MELPNIMHPVAKLSTALAAALM LSGC MPGEIRPTIGQQMETGDQRFGDL 49
NDM-14 1 MELPNIMHPVAKLSTALAAALM LSGC MPGEIRPTIGQQMETGDQRFGDL 49
NDM-15 1 MELPNIMHPVAKLSTALAAALM LSGC MPGEIRPTIGQQMETGDQRFGDL 49
NDM-16 1 MELPNIMHPVAKLSTALAAALM LSGC MPGEIRPTIGQQMETGDQRFGDL 49
*****

```

Supplementary Figure 9. All NDM variants have a conserved lipobox. Sequence alignment of N-terminus of NDM-1 to NDM-16. Conserved LSGC lipobox sequences and residues at +2 position are shown in red and green, respectively. Alignment was performed with the T-Coffee tool, available at www.tcoffee.org.



Supplementary Figure 10. Lipoproteins are present in all MBL subclasses.

Phylogenetic trees of B1+B2 (**a**) and B3 (**b**) characterized MBLs, together with homologues harbouring a lipidation site in their N-termini (gi accession numbers). Lipoproteins are shown in red and characterized soluble MBLs in black. Trees were calculated from structure-assisted multiple sequence alignments with LG substitution model and 100 bootstraps, using the maximum likelihood algorithm PhyML (see Methods section for details).

Figure 1b

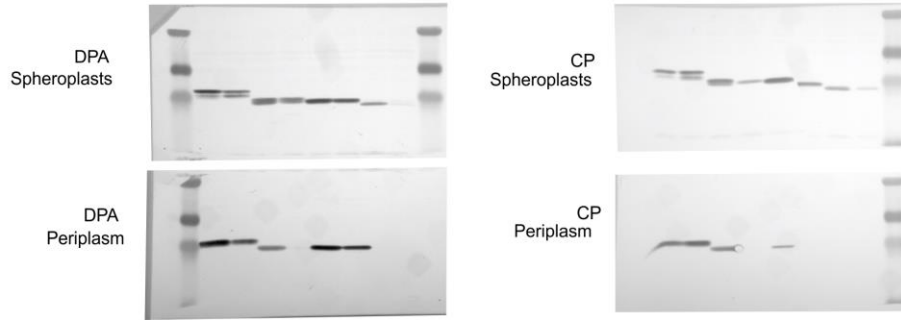


Figure 2a

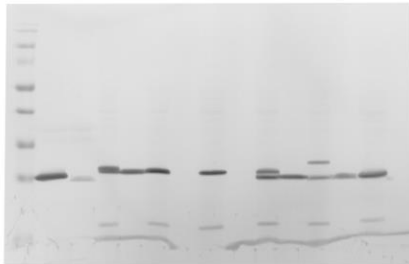


Figure 2c

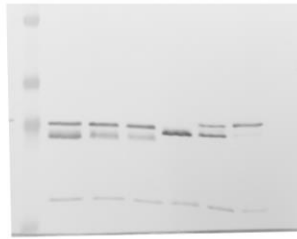


Figure 3d

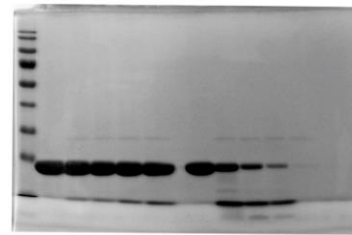


Figure 4b

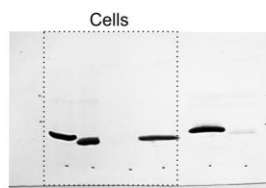
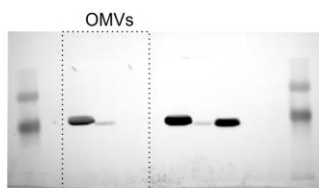


Figure 4c

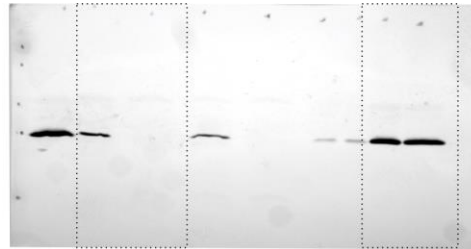


Figure 4f

Figure 5c

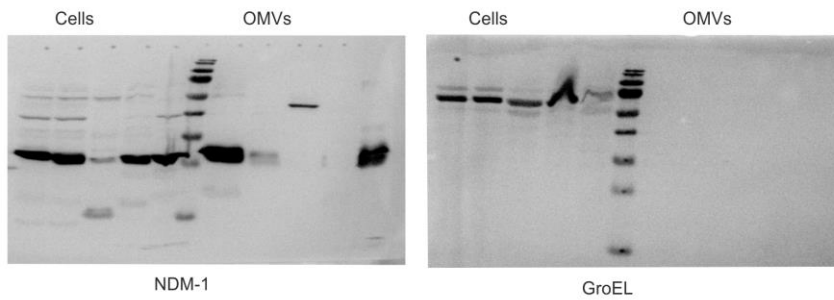
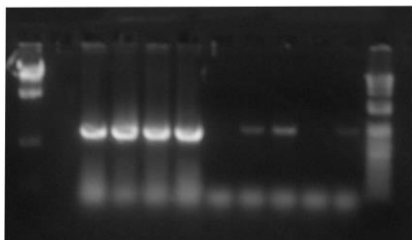
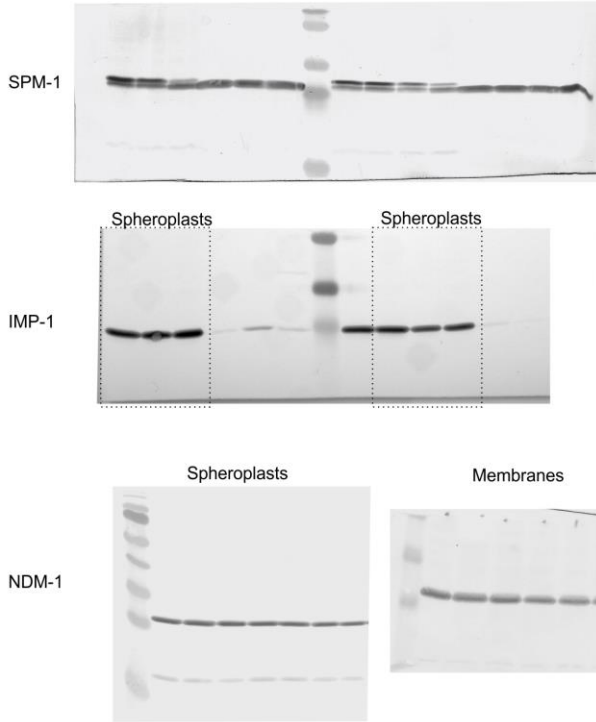


Figure 5d

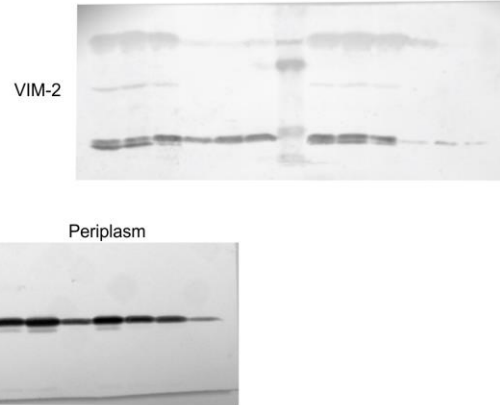


Supplementary Figure 11. Full, uncut gel images for Figures 1, 2, 3, 4 and 5.

Supplementary Figure 1b

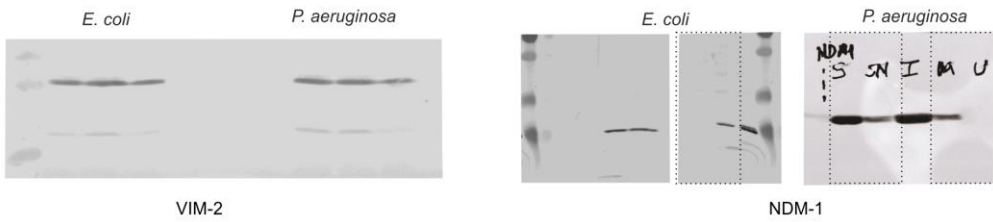


Supplementary Figures 1b, 5 and 6b

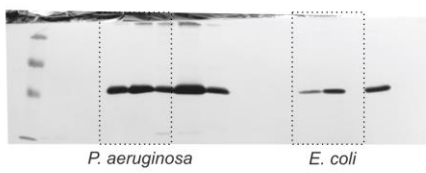


Supplementary Figures 1b and 6b

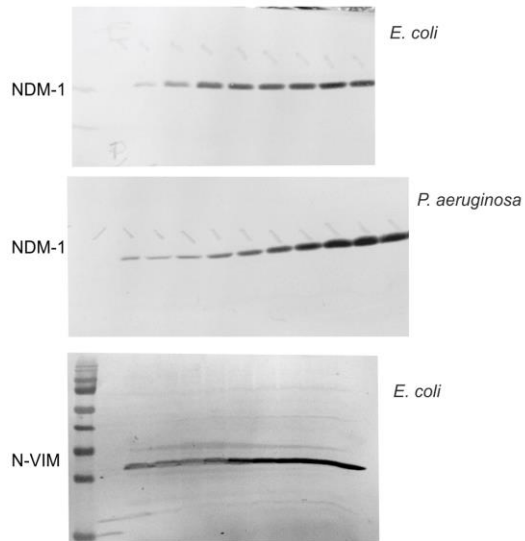
Supplementary Figure 3a



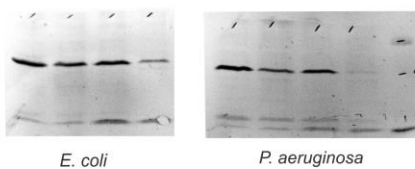
Supplementary Figure 3b



Supplementary Figure 4a-b

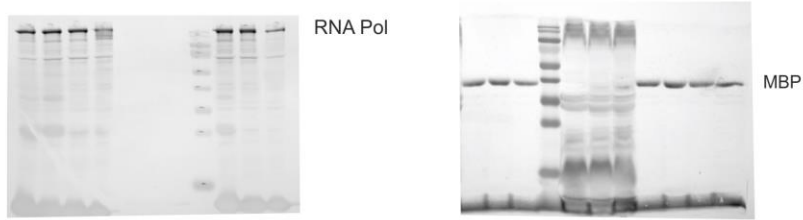


Supplementary Figure 4c

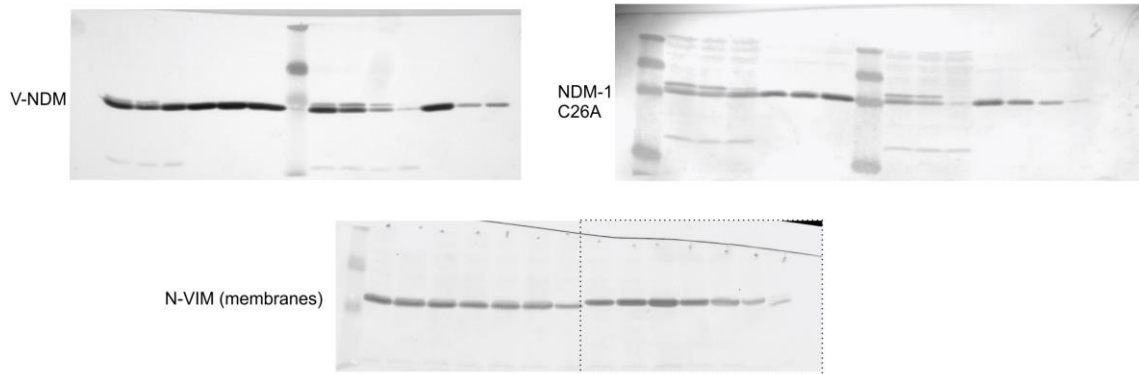


Supplementary Figure 12. Full, uncut gel images for Supplementary Figures 1, 3, 4, 5 and 6.

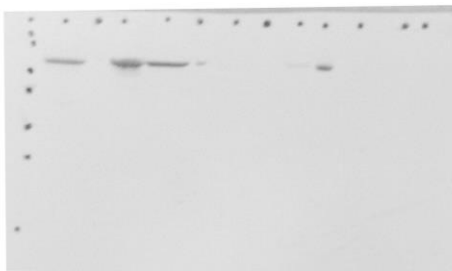
Supplementary Figure 5



Supplementary Figure 6b



Supplementary Figure 7



Supplementary Figure 13. Full, uncut gel images for Supplementary Figures 5, 6 and 7.

	Imipenem MIC ($\mu\text{g/mL}$)											
	0 μM DPA		200 μM DPA		350 μM DPA		500 μM DPA		750 μM DPA		1000 μM DPA	
	WT	+ST	WT	+ST	WT	+ST	WT	+ST	WT	+ST	WT	+ST
pMBLe (control)	0.25		0.25		0.25		0.25		0.25		0.125	
NDM-1	2	2	1-2	1-2	0.5-1	0.5-1	0.5	0.5	0.25	0.25	0.125	0.125
VIM-2	2	2	1	1	0.25-0.5	0.25-0.5	0.25	0.25	0.25	0.25	0.125	0.125
IMP-1	1	1	1	1	0.5	0.5	0.5	0.5	0.25	0.25	0.125	0.125
SPM-1	2	2	2	2	1	1	1	1	0.5	0.5	0.125	0.125

Supplementary Table 1. Imipenem MICs of *E. coli* cells expressing wild type (WT) and C-terminal strep-tagged (+ST) variants of MBLs, as a function of extracellular Zn(II) availability. Values were determined by triplicate.

	Imipenem MIC ($\mu\text{g/mL}$)						
	0 μM DPA	200 μM DPA	350 μM DPA	500 μM DPA	750 μM DPA	1000 μM DPA	
pMBLe (control)	0.25	0.25	0.25	0.25	0.25	0.125	
NDM-1	2	1-2	0.5-1	0.5	0.25	0.125	
NDM-1 C26A	2	1	0.5	0.25	0.25	0.125	
V-NDM	4-8	1	0.5	0.25	0.25	0.125	
VIM-2	2	1	0.25-0.5	0.25	0.25	0.125	
N-VIM	0.5	0.25	0.25	0.25	0.25	0.125	
IMP-1	1	1	0.5	0.5	0.25	0.125	
SPM-1	2	2	1	1	0.5	0.125	

	Cefotaxime MIC ($\mu\text{g/mL}$)						
	0 μM DPA	200 μM DPA	350 μM DPA	500 μM DPA	750 μM DPA	1000 μM DPA	
pMBLe (control)	0.06	0.06	0.06	0.06	0.06	0.06	
NDM-1	8	8	2	2	0.25	0.06	
NDM-1 C26A	8-16	8	2	1	0.125	0.06	
V-NDM	64	8	2	0.5	0.06-0.125	0.06	
VIM-2	4-8	4-8	2	0.5	0.06-0.125	0.06	
N-VIM	0.5	0.125	0.06	0.06	0.06	0.06	
IMP-1	2-4	2-4	2	1-2	0.5	0.125	
SPM-1	128	128	128	64-128	32	4	

Supplementary Table 2. Imipenem and cefotaxime MICs of *E. coli* cells expressing different MBLs as a function of extracellular Zn(II) availability. Values were determined by triplicate.

	MIC ($\mu\text{g/mL}$)				
	Imipenem	Cefotaxime	Piperacillin	Cefepime	Ceftazidime
pMBLe (control)	0.25	0.06	1	0.03	0.125-0.25
VIM-2	2	4-8	32-64	0.25-0.5	8
N-VIM	0.5	0.5	8	0.03-0.06	0.5
NDM-1	2	8	32-64	4-8	256
V-NDM	4-8	64	256	16-32	1024-2048
NDM-1 C26A	2	16	64	8-16	512

Supplementary Table 3. β -lactam antibiotics MIC values for *E. coli* expressing VIM-2, NDM-1 and mutant variants. Values were determined by triplicate.

	Imipenem MIC ($\mu\text{g/mL}$)		
	0 $\mu\text{g/mL}$ CP	100 $\mu\text{g/mL}$ CP	300 $\mu\text{g/mL}$ CP
pMBLe (control)	0.125	0.125	0.125
NDM-1	1	1	0.125
NDM-1 C26A	2	1	0.125
V-NDM	4	2	0.125
N-VIM	0.125-0.25	0.125	0.125
VIM-2	2	2	0.125

Supplementary Table 4. Imipenem MICs for *E. coli* expressing VIM-2, NDM-1 and mutant variants, in presence of calprotectin. Values correspond to three independent replicates.

MBL subclass	Name	Genbank GI number	Confirmed lactamase activity?	Lipobox sequence (including +2)	Organism	
B1	NDM-1	GI:255031063	yes	LSGCM	<i>Klebsiella pneumoniae</i>	
	380732286	GI:380732286	no	LTACA	<i>Coralloccoccus coralloides</i>	
	636675015	GI:636675015	yes ²	IVACA	Uncultured organism	
	648605020	GI:648605020	no	LSGCA	<i>Hirschia maritima</i>	
	254043948	GI:254043948	no	LSGCM	<i>Hirschia báltica</i>	
	499733708	GI:499733708	yes ³	LPACV	<i>Erythrobacter litoralis</i>	
	495875539	GI:495875539	no	VAGCT	<i>Alpha proteobacterium JLT2015</i>	
	505205117	GI:505205117	no	LIACS	<i>Clostridium saccharoperbutylacetonicum</i>	
	167775165	GI:167775165	no	VSGCQ	<i>Leptospira biflexa</i>	
	511022315	GI:511022315	no	LTGCS	<i>Bacteroides massiliensis</i>	
	254966891	GI:254966891	yes ⁴	LTGCT	Uncultured organism	
	522024102	GI:522024102	no	LVGCS	<i>Lewinella cohaerens</i>	
	88707419	GI:88707419	no	LIIGC	<i>Maribacter</i> sp.	
	498202808	GI:498202808	no	LTSCK	<i>Mesoflavibacter zeaxanthinifaciens</i>	
	657645513	GI:657645513	no	ITGCK	<i>Cellulophaga baltica</i>	
	657642553	GI:657642553	no	ITGCK	<i>Cellulophaga baltica</i>	
	499127206	GI:499127206	no	LAGCS	<i>Cyclobacteriaceae bacterium AK24</i>	
	522022580	GI:522022580	no	IIGCT	<i>Flexithrix dorotheae</i>	
	532760610	GI:532760610	no	LSSCI	Uncultured organism	
	636673149	GI:636673149	yes ²	IVACC	Uncultured organism	
	636669520	GI:636669520	yes ²	LASCA	Uncultured organism	
	636669920	GI:636669920	yes ²	LASCA	Uncultured organism	
	636669520	GI:636669520	yes ²	LASCA	Uncultured organism	
	636677946	GI:636677946	yes ²	LAGCT	Uncultured organism	
	636668516	GI:636668516	yes ²	LSSCS	Uncultured organism	
	B2	SfhI	GI:639192216	yes ⁵	LIACE	<i>Serratia fonticola</i>
	B3	EAM-1	GI:396086049	yes ⁶	IAACA	<i>Erythrobacter aquimaris</i>
		EVM-1	GI:396086043	yes ⁶	LSGCA	<i>Erythrobacter vulgaris</i>
		ECM-1	GI:396086047	yes ⁶	LAGCA	<i>Erythrobacter citreus</i>
		EFM-1	GI:396086041	yes ⁶	LAACA	<i>Erythrobacter flavus</i>
		627787923	GI:627787923	no	LAACR	<i>Stenotrophomonas rhizophila</i>
		601091642	GI:601091642	no	LAACA	<i>Lysobacter capsici</i> AZ78
		518294332	GI:518294332	no	LSACL	<i>Dyella japonica</i>
662145257		GI:662145257	no	VAGCT	<i>Mycobacterium abscessus</i>	
GOB-11		GI:49798147	yes ⁷	LSACL	<i>Elizabethkingia meningoseptica</i>	
444243241		GI:444243241	yes ⁸	VIGCA	Uncultured organism	
496318736		GI:496318736	no	LAACP	<i>Bradyrhizobium</i> sp. ORS 375	
654343527		GI:654343527	no	LAACS	<i>Mastigocoleus testarum</i>	
563281132		GI:563281132	no	VSSCA	<i>Blastomonas</i> sp. CACIA14H2	
665869717		GI:665869717	no	LVGCA	<i>Asticcacaulis</i> sp. AC460	
493317888		GI:493317888	no	LAGCT	<i>Asticcacaulis biprosthecium</i>	
636671861		GI:636671861	yes ²	VSSCA	Uncultured organism	
495496401	GI:495496401	no	LAGCS	<i>Rheinheimera nanhaiensis</i>		
660647583	GI:660647583	no	LAGCS	<i>Erythrobacter</i> sp. JL475		

Supplementary Table 5. MBL lipoproteins from B1, B2 and B3 subclasses.

Predicted MBL lipoproteins harbouring a consensus lipobox sequence [LVI][ASTVI][GAS][C] in the N-terminus, obtained as described in Methods section.

Supplementary Information References

- 1 Kovacs-Simon, A., Titball, R. W. & Michell, S. L. Lipoproteins of bacterial pathogens. *Infect. Immun.* **79**, 548-561 (2011).
- 2 Forsberg, K. J. *et al.* Bacterial phylogeny structures soil resistomes across habitats. *Nature* **509**, 612–616 (2014).
- 3 Zheng, B. *et al.*, An unexpected similarity between antibiotic-resistant NDM-1 and β -lactamase II from *Erythrobacter litoralis*. *Protein Cell* **2**, 250-258 (2011).
- 4 Sommer, M. O. A., Dantas, G. & Church, G. M. Functional Characterization of the Antibiotic Resistance Reservoir in the Human Microflora. *Science* **325**, 1128-1131 (2009).
- 5 Saavedra, M. J. *et al.* Sfh-I, a subclass B2 metallo- β -lactamase from a *Serratia fonticola* environmental isolate. *Antimicrob. Agents Chemother.* **47**, 2330-2333 (2003).
- 6 Girlich, D., Poirel, L. & Nordmann, P. Diversity of naturally occurring Ambler class B metallo- β -lactamases in *Erythrobacter spp.* *J. Antimicrob. Agents Chemother.* **67**, 2661-2664 (2012).
- 7 Yum, J. H. *et al.* Genetic diversity of chromosomal metallo- β -lactamase genes in clinical isolates of *Elizabethkingia meningoseptica* from Korea. *J. Microbiol.* **48**, 358-64 (2010).
- 8 Terrón-González, L., Medina, C., Limón-Mortés, M. C. & Santero, E. Heterologous viral expression systems in fosmid vectors increase the functional analysis potential of metagenomic libraries. *Sci. Rep.* **3**, 1107 (2013).